

Colorimetric detection of lead (II) based on silver nanoparticles capped with iminodiacetic acid

Li Qi · Yan Shang · Fangying Wu

Received: 3 February 2012 / Accepted: 9 May 2012 / Published online: 24 May 2012
© Springer-Verlag 2012

Abstract We report on a colorimetric probe for the determination of Pb(II). It is based on the use of silver nanoparticles that have been functionalized with iminodiacetic acid (IDA-Ag NPs). The absorption spectrum and solution color of IDA-Ag NPs undergo dramatic changes on exposure to Pb(II) with a new absorption peak appearing at 650 nm and a concomitant color change from yellow to green. This is assumed to result from the aggregation of IDA-Ag NPs induced by Pb(II). Under optimum conditions, there is a linear relationship between the ratio of the absorbances at 650 and 396 nm, respectively, and the concentration of Pb(II) in the 0.4 to 8.0 μM concentration range, with a detection limit of 13 nM. The method was applied to the determination of Pb(II) in tap water and urea samples, and recoveries ranged from 93.7 % to 98.6 %.

Keywords Silver nanoparticles · Aggregation · Colorimetric probe · Iminodiacetic acid · Lead ion

Introduction

The wide use of lead in the fields of electric storage batteries, gasoline additives, paint pigments, pipes, ammunition, soldering activities, etc., for many years is attributed to its abundant physical properties. Thus, its wide usage makes lead one of the most important pollutants [1, 2]. Lead poisoning can cause a variety of diseases, such as muscle

paralysis, memory loss, irritability, and anemia [3–5]. Therefore, developing rapid and sensitive methods to detect trace Pb^{2+} is crucial. Currently, many analytical methods to determine trace Pb^{2+} have been developed. The common methods used to detect Pb^{2+} include atomic absorption spectrometry [6] and inductively coupled plasma optical emission spectrometry [7]. Nevertheless, these techniques are expensive, time-consuming, and require special laboratories. Colorimetric assay has received attentions because it can avoid these limitations [8, 9]. Moreover, the detection signal can be viewed by the naked eyes [10, 11]. Silver and gold nanoparticles are frequently employed as colorimetric probes for sensing biomolecules and metal ions because of their distance-dependent optical properties and extremely high extinction coefficients [12–16]. When ligands assembled on the surface of nanoparticles bond with an analyte, the aggregation of nanoparticles occurs. Consequently, the changes in color and absorption spectrum can be observed. Thus, the surface modification of nanoparticles is very important to improve the stability and sensing selectivity of nanoparticles [17–20]. For example, Li and his group synthesized glutathione-stabilized silver nanoparticles as colorimetric sensors for nickel ion [21] and aza-crown ether-modified silver nanoparticles as colorimetric sensors for Ba^{2+} [22]. Huang and his group reported polythymine-stabilized gold nanoparticles for the recognition of melamine [23]. Takarda and his group developed double-stranded DNA-carrying gold nanoparticles for detection of mercury ion [24]. Recently, Chai and his group [9] have reported glutathione modified gold nanoparticles based colorimetric assay for the detection of Pb^{2+} at 20 ppb level. Ray and his group also have reported glutathione conjugated gold nanoparticles probe for detection of Pb^{2+} from plastic toys, paints, and water samples [25].

Iminodiacetic acid (IDA) possesses not only good water-solubility but also strong binding ability with metal ions. In

Electronic supplementary material The online version of this article (doi:10.1007/s00604-012-0832-3) contains supplementary material, which is available to authorized users.

L. Qi · Y. Shang · F. Wu (✉)
Department of Chemistry, Nanchang University,
Nanchang 330031, China
e-mail: fywu@ncu.edu.cn

view of this, IDA and its derivatives have been employed to modify the surface of nanoparticles to sense metal ions effectively [26]. In the current study, we report a colorimetric assay for the determination of Pb^{2+} in aqueous solution based on Ag NPs coated with iminodiacetic acid. The functionalized IDA-Ag NPs was induced to aggregate in the presence of Pb^{2+} through electrostatic and metal-ligand interactions. Scheme 1 depicts the mechanism for the color change of Ag NPs induced by Pb^{2+} .

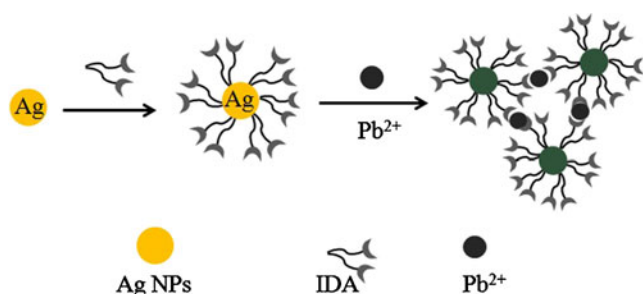
Experimental

Materials

All chemicals were of analytical grade and used without further purification. All solutions were prepared using doubly distilled water. IDA is a product of Sigma-Aldrich Corp. (USA, <http://www.sigmaaldrich.com>). Silver nitrate (AgNO_3), sodium borohydride (NaBH_4), and the other metallic ions were purchased from Shanghai Qingxi Technology Co., Ltd. (Shanghai, China, www.ce-r.cn/sites/qingxi/).

Instruments

Absorption spectra were recorded on a UV–vis 2550 spectrophotometer (Shimadzu, Japan, www.shimadzu.com) using a 1.0 cm quartz cell. Infrared spectra were obtained with KBr pellets on a Nicolet 5700 FTIR spectrometer (Nicolet, USA, www.thermonicolet.com). Transmission electron microscopy (TEM) images were acquired on a JEM-2010 transmission electron microscope (JEOL Ltd. Japan, <http://www.jeol.cn>). Size distribution and zeta potential of IDA-Ag NPs in different pH value media were measured on a Hydrosol Nanoparticle Size Analyzer and Zeta Potential Analyzer (PSA NANO2590, Malvern Companies, UK, www.malvern.com). All pH measurements were made using a pHS-3 digital pH-meter (Shanghai REX Instrument Corp., Shanghai, China, <http://en.lei-ci.com>) combined with a glass-calomel electrode.



Scheme 1 Pb^{2+} -induced the aggregation of IDA-Ag NPs resulting colorimetric responses

Preparation of IDA-Ag NPs and bare Ag NPs

IDA-Ag NPs were prepared through the method reported previously [27]. Briefly, 2.0 mL AgNO_3 aqueous solution (0.01 mol L^{-1}) mixed with 2.0 mL IDA (0.01 mol L^{-1}) was diluted to 100 mL with doubly distilled water respectively. After 15 min, the solution added with sodium borohydride (NaBH_4 , 8.8 mg) reduced quickly under vigorous shaking. The mixture was stirred for 2 h in the dark at room temperature; bright yellow silver colloids were then obtained. The IDA-modified Ag NPs were used in the following experiments without further purification. The bare Ag NPs were prepared in the same way without IDA.

Results and discussion

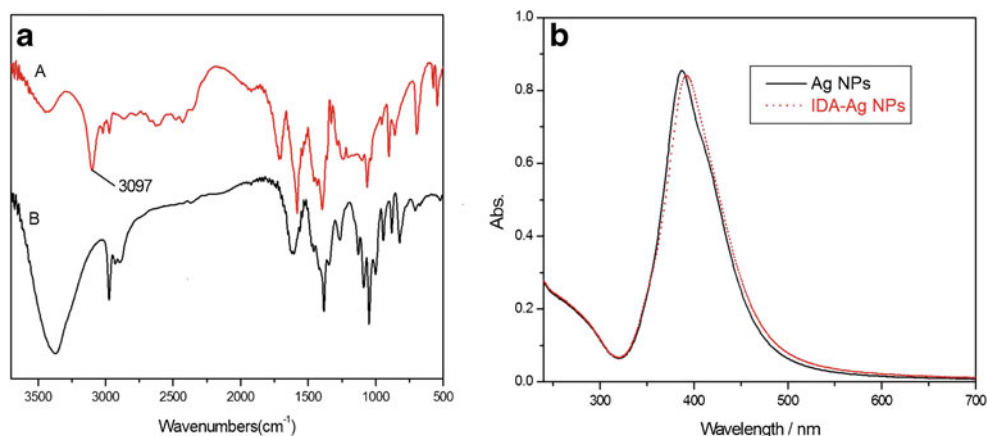
Characterization of IDA-Ag NPs

Figure 1 shows the infrared and absorption spectra of pure IDA and IDA-Ag NPs. Comparing the IR spectra of them, significant features were observed: the characteristic peak of N-H located at 3100 cm^{-1} disappeared, indicating that IDA modified onto the surface of Ag NPs. View from Fig. 1b, it is clear that the absorption spectrum of IDA-Ag NPs underwent a little red-shift compared with that of bare Ag NPs, which also demonstrates that IDA modified onto the surface of Ag NPs. Similar spectral changes were found in Ag NPs modified with bipyridine [27–29]. It has been proved that the adsorption of organic compounds on the metal nanoparticles resulted in a red shift in the SPR band, mainly caused by the lessening of the plasma oscillation frequency or a change in the dielectric constant of the microenvironment around the nanoparticles.

Stability and size of IDA-Ag NPs

The prepared Ag NPs solution modified with IDA was stable and highly dispersed. The TEM image of IDA-Ag NPs was obtained, as shown in part a of Fig. 2. Clearly, IDA-Ag NPs were highly dispersed in aqueous solution, with the size estimated as 8 nm. The size distribution of IDA-Ag NPs was also studied and presented in Fig. S1 (Electronic Supplementary Material, ESM). The size of 82 % IDA-Ag NPs particles was about 7 to 10 nm, which concurred with the appearance size of the TEM result. Further, note that, even if the solution was maintained for 30 days in $4 \text{ }^\circ\text{C}$ in a refrigerator, the graph of the size distribution changed little. Thus, we conclude that IDA-Ag NPs are highly dispersed and stabilized, making them promising for further application.

Fig. 1 **a** FT-IR spectra of IDA (A) and IDA-Ag NPs(B) with KBr pellets, **b** Absorption spectra of bare Ag NPs and IDA-Ag NPs in aqueous solution



Optimal experimental condition

Effect of IDA concentration

The IDA concentration not only affects the stability of the Ag NPs, but also affects the determination of the sensitivity. The optical IDA concentration was studied and the results showed in Fig. S2 (ESM). When the IDA concentration is low, it is very sensitive for detection smaller amounts of Pb^{2+} . However, the concentration of IDA can't be too low because the Ag NPs are not stable with less IDA and are aggregated by themselves. Meanwhile, the experiment results also display the size of IDA-Ag NPs increase little while the concentration of IDA increased (seen Fig. S1, ESM). So in this system, the molar concentration ratio of Ag^+ / IDA was fixed at 1:1.

Effect of pH value on absorption spectrum of IDA-Ag NPs

The effect of pH value on the absorption spectrum of IDA-Ag NPs was investigated in our current work and shown in Fig. S4 (ESM). The results display the nanoparticles are

considered stable at a pH range of 3.0 to 12.0 and are extremely stable at pH 5.0 to 9.0. Reportedly, the pKa of IDA are 2.98 and 9.89 [30]. The carboxyl groups of IDA are unprotonated and negatively charged, indicating that IDA-Ag NPs are charged particles under these pH conditions which is supported by the zeta potential (seen Fig. S4, ESM). Thus, the electrostatic force of nanoparticles surfaces was assumed the reason why nanoparticles were stable in this pH range.

Effect of reaction time on IDA-Ag NPs aggregation induced by Pb^{2+}

The aggregation kinetics of our assay was examined with different concentration of Pb^{2+} by measuring the absorbance of IDA-Ag NPs at 650 nm at room temperature. Fig. S5 (ESM) shows that the absorbance of IDA-Ag NPs at 650 nm increased and then stabilized within 2 min after the addition of Pb^{2+} . In other words, the aggregation of the IDA-Ag NPs occurred immediately after the addition of Pb^{2+} , which was consequently completed in 2 min. Thus, the method was enabled to rapid detection of Pb^{2+} in water samples.

Fig. 2 TEM images of dispersed IDA-Ag NPs (a) and aggregated IDA-Ag NPs induced by Pb^{2+} (b)

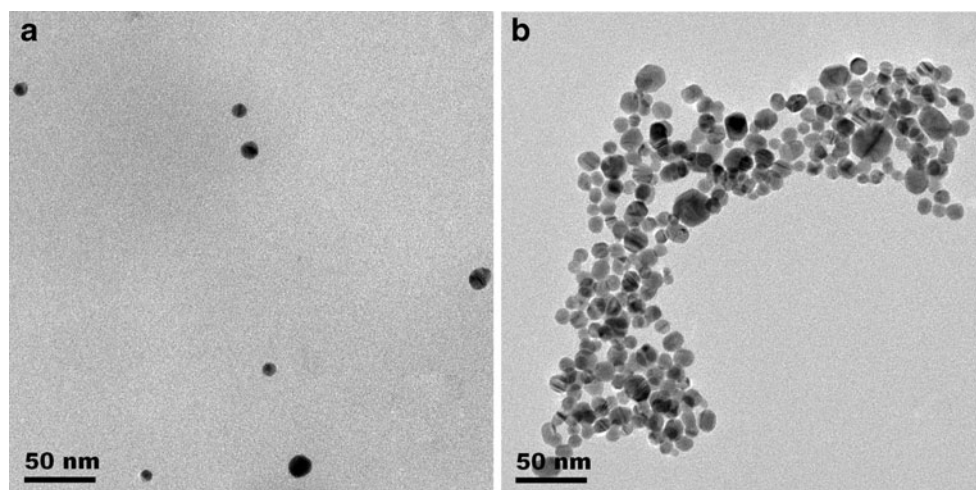
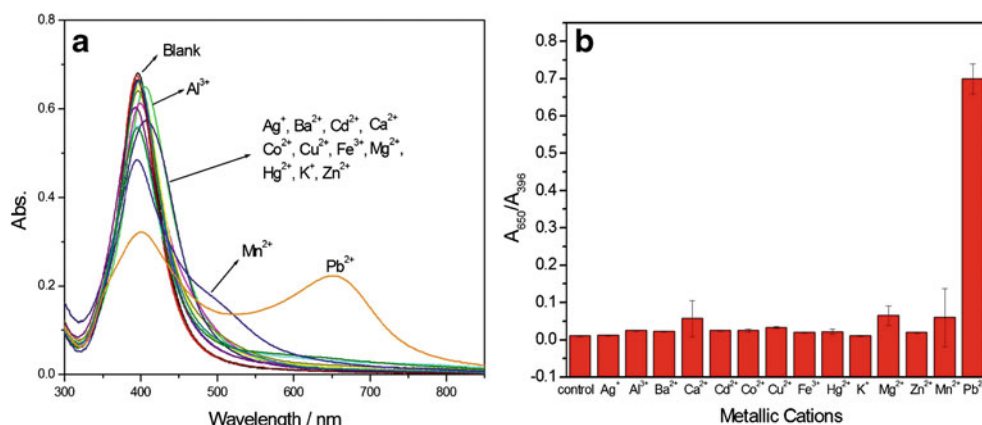


Fig. 3 UV–vis absorption spectra (a) and intensity ratio of $A_{650\text{nm}}/A_{396\text{nm}}$ (b) of Ag NPs solution after mixing with $10\ \mu\text{M}\ \text{Pb}^{2+}$ and other metal ions ($10\ \mu\text{M}$ for Mn^{2+} , $20\ \mu\text{M}$ for Cd^{2+} , Cu^{2+} , Hg^{2+} , Ba^{2+} , $100\ \mu\text{M}$ for Ca^{2+} , Zn^{2+} and $200\ \mu\text{M}$ for Co^{2+} , Li^+ , Ag^+ , Fe^{3+} , Mg^{2+} , K^+ , Ca^{2+} , Al^{3+}) in pH 8 aqueous solution, respectively



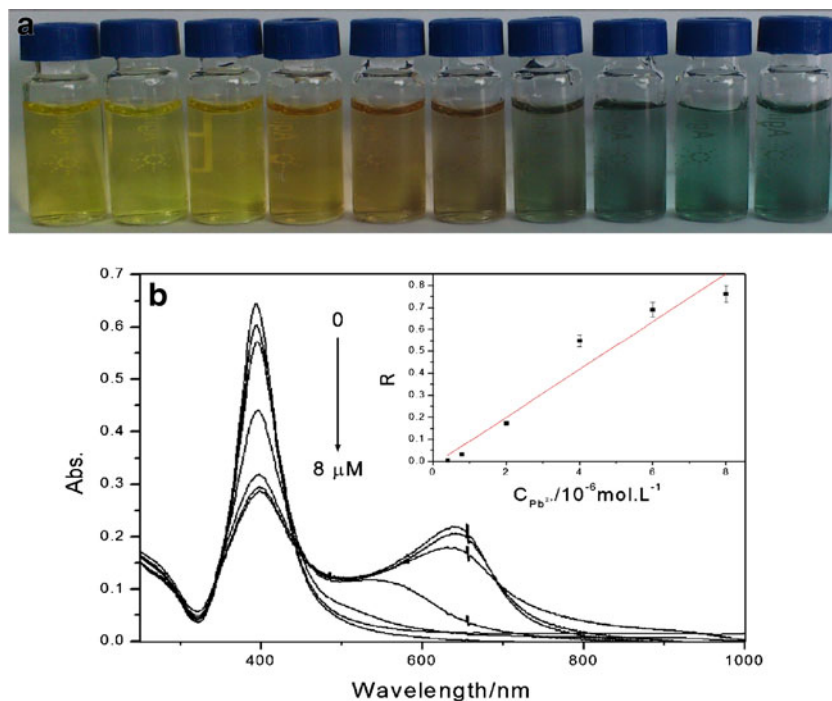
Metal ion recognition based on IDA-Ag NPs

To investigate the recognition ability of IDA-Ag NPs with metal ions, the absorption titration of IDA-Ag-NPs against 15 metal ions, including Pb^{2+} , Cd^{2+} , Cu^{2+} , Ba^{2+} , Ca^{2+} , Zn^{2+} , Co^{2+} , Mn^{2+} , Ag^+ , Fe^{3+} , Mg^{2+} , Hg^{2+} , K^+ , Ca^{2+} , and Al^{3+} , was performed respectively. Upon interaction with various metal ions, both the absorption spectral changes and the absorbance ratio A_{650}/A_{396} changes of IDA-Ag NPs are presented in Fig. 3. As shown Fig. 3a, the maximum absorption wavelength of IDA-Ag NPs peaked at 396 nm, and the presence of $10\ \mu\text{M}\ \text{Pb}^{2+}$ caused the spectrum to change dramatically. The absorbance at 396 nm decreased, and a new absorption band appeared at approximately 650 nm, along with the color change from yellow to green. However, upon the addition of other metal ions, such as Cd^{2+} , Cu^{2+} , Ba^{2+} , Ca^{2+} , Zn^{2+} , Co^{2+} , Ag^+ , Fe^{3+} , Mg^{2+} , Hg^{2+} , K^+ , Ca^{2+} , and Al^{3+} , the absorbance at 396 nm showed slight

changes, and a new absorbance band did not appear. Only the concentration of Mn^{2+} was higher than $20\ \mu\text{M}$, a new absorption peak would be found at about 570 nm. Figure 3b displays the intensity ratio of $A_{650\text{nm}}/A_{396\text{nm}}$ of IDA-Ag NPs when added with various metal ions. Clearly, IDA-Ag-NPs show high selectivity on Pb^{2+} over other ions.

To evaluate the sensitivity of Pb^{2+} dependent on the colorimetric assay under the optimized detection conditions, the color change of the IDA-Ag NPs solution was recorded by digital camera, the absorption spectral change was monitored by UV–vis spectroscopy. The absorption spectral and solution color changes of IDA-Ag NPs upon the addition of Pb^{2+} are presented in Fig. 4. Figure 4a shows the color changes in IDA-Ag NPs after the addition of different concentrations of Pb^{2+} . As the concentration of Pb^{2+} increased, the color of IDA-Ag NPs solution changed from yellow to yellow brown, yellow green, and deep green, which could be easily observed by naked eyes. Such changes can be

Fig. 4 a Color changes in IDA-Ag NPs solution after the addition of different concentrations of Pb^{2+} ions. b The absorption spectra of Ag NPs solution with various concentrations of Pb^{2+} were 0, 0.4, 0.8, 2, 4, 6, and $8 \times 10^{-6}\ \text{M}$, respectively. The inset shows the dependence of $R(A_{650}/A_{396})$ values of IDA-Ag NPs on increasing concentration of Pb^{2+}



easily used as a quantitative assay for trace Pb^{2+} . Figure 4b illustrates the absorption spectral change of IDA-Ag NPs in the presence and absence of Pb^{2+} . Upon the addition of increasing Pb^{2+} , the absorbance at 396 nm decreased, and a new absorption peak appeared progressively at a longer wavelength range. Finally, the new absorption band red shifted to 650 nm, with the increasing concentration of Pb^{2+} maintained.

A good linear relationship between intensity ratio A_{650}/A_{396} and the concentration of Pb^{2+} ranging from 0.4 μM to 8.0 μM was also obtained (seen in the inset plot of Fig. 4b). The regression equation was $A_{650}/A_{396} = -0.019 + 1.1 \times 10^5 \times C_{\text{Pb}} (\text{mol L}^{-1})$. The limit of detection (LOD) was given as 13 nM by equation $\text{LOD} = K \times S_0/S$, where K is a numerical factor chosen according to the confidence level desired, S_0 is the standard deviation (SD) of the blank measurements ($n=13$, $K=3$), and S is the slope of the calibration curve. Based on the investigation, a simple colorimetric assay of Pb^{2+} was introduced. Some similar methods for determination lead were listed in the Table 1. It is clear that the determination wavelength and the limit of detection of proposed method are better compared with the other methods.

Analysis of real samples

To validate the reliability of our method, the detection of Pb^{2+} was performed in tap water and urea sample. The results are presented in Table 2. It is found that the Pb^{2+} content in the tested samples is too low to be detected by the IDA-Ag NPs. However, there is an obvious signal can be readout if different concentrations of Pb^{2+} are added into the sample. The mean recovery was 93.7 % to 98.6 %, and RSD was about 1.2–5.4 %.

Mechanism

The spectral and color changes could be explained well by the aggregation of Ag NPs through the electrostatic

Table 1 Comparison of analytical parameters of different methods for determination of Pb^{2+}

Reagent	Monitor wavelengths	Linear range	Detection limit	Reference
GSH-GNPs	700 nm, 520 nm	0.1–50 μM	100 nM	[9]
2-mercaptoethanol - Au NPs- Na_2S	650 nm, 520 nm	50–500 nM	45 nM	[31]
G/C-AuNPs	610 nm, 521 nm 538 nm	1–10 μM 2.9–37.7 fM	1 μM –	[32]
DNAzyme-directed assembly of gold nanoparticles	522 nm, 700 nm	0.1–4 μM 10–200 μM	–	[33]
IDA-Ag NPs	650 nm, 396 nm	0.4–8.0 μM	13 nM	This work

Table 2 Determination of Pb^{2+} in tap water and urea sample by the standard addition method

Sample	Detection ($10^{-7} \text{ mol L}^{-1}$)	Added ($10^{-7} \text{ mol L}^{-1}$)	Found ($n=3$) ($10^{-7} \text{ mol L}^{-1}$)	Recovery (%)	RSD/%
Tap water	Not found	6.5	6.1	93.8	1.8
		8.0	7.5	93.7	1.7
urea sample	Not found	7.0	6.9	98.6	1.2
		16.0	15.5	96.9	5.4

interaction between Pb^{2+} and carboxylate anion of the IDA. The IDA-Ag NPs were stabilized in the solution because the IDA on the surface of Ag NPs protected them from aggregation. IDA has two free—COOH groups and one—NH group, which can be used to bind with metal ions. In our current assay, IDA is linked with Ag NPs through—NH linkage and as a result, there is no free—NH groups for the formation of complex with metal ions like, Fe^{2+} , Zn^{2+} , and Cd^{2+} which are well-known to bind to amino group [34, 35]. As a result,—COOH is the only binding site, which is known to bind strongly with Pb^{2+} [25, 34]. In the presence of Pb^{2+} , negative carboxylate anion of IDA functionalized on the nanoparticles' surface can be attracted together through a carboxylate- Pb^{2+} -carboxylate linker at pH 8. The bridging interactions between Pb^{2+} and IDA can also be identified by the fact that the colorimetric change did not occur in the presence of EDTA (Fig. 5), which is a well-known strong chelator for divalent cations. Similar observation has been found in the reported references [11, 36, 37]. Based on interactions between carboxylate and Pb^{2+} , the neighboring Ag NPs became closer and finally aggregated. The aggregation of IDA-Ag NPs was also confirmed by TEM (seen the part B of Fig. 2). The TEM image shows IDA-Ag NPs were dispersed uniformly in aqueous solution. The aggregation was clearly observed when Pb^{2+} was added into the solution.

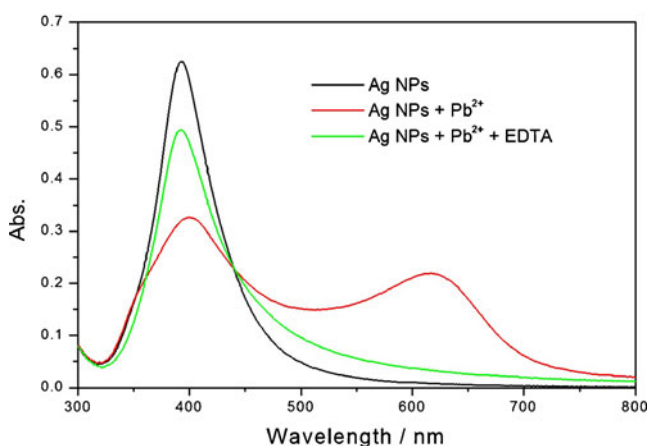


Fig. 5 Reversible binding of Pb^{2+} with IDA-Ag NPs in the presence of EDTA

Conclusion

In summary, a low-cost, simple and fast colorimetric platform for the specific detection of trace Pb^{2+} using functionalized Ag NPs was introduced. The interaction between IDA capped on Ag-NPs and Pb^{2+} plays a key role in the aggregation of Ag-NPs. Thus, the selection and construction of modifier can significantly improve the selectivity of probes.

Acknowledgements Financial supports from Natural Science Foundation of China (no. 20965006) are highly acknowledged.

References

- Lanphear BP (1998) The paradox of lead poisoning prevention. *Science* 281:1617
- Lanphear BP, Roghmann KJ (1997) Pathways of lead exposure in urban children. *Environ Res* 74:67
- Strużyńska L, Walski M, Gadamski R, Dabrowska-Bouta B, Rafałowska U (1997) Lead-induced abnormalities in blood-brain barrier permeability in experimental chronic toxicity. *Mol Chem Neuropathol* 31:207
- Rifai N, Cohen G, Wolf M, Cohen L, Faser C, Savory J, DePalma L (1993) Incidence of lead poisoning in young children from inner-city, suburban, and rural communities. *Ther Drug Monit* 15:71
- Needleman H (2004) Lead poisoning. *Annu Rev Med* 55:209
- Soylak M, Cay RS (2007) Separation/preconcentration of silver(I) and lead(II) in environmental samples on cellulose nitrate membrane filter prior to their flame atomic absorption spectrometric determinations. *J Hazard Mater* 146:142
- MdGA K, de Andrade JB, de Jesus DS, Lemos VA, Bandeira MLSF, dos Santos WNL, Bezerra MA, Amorim FAC, Souza AS, Ferreira SLC (2006) Separation and preconcentration procedures for the determination of lead using spectrometric techniques: a review. *Talanta* 69:16
- Liu J, Lu Y (2006) Preparation of aptamer-linked gold nanoparticle purple aggregates for colorimetric sensing of analytes. *Nat Protoc* 1:246
- Chai F, Wang C, Wang T, Li L, Su Z (2010) Colorimetric detection of Pb^{2+} using glutathione functionalized gold nanoparticles. *ACS Appl Mater Inter* 2:1466
- Xue Y, Zhao H, Wu Z, Li X, He Y, Yuan Z (2011) Colorimetric detection of Cd^{2+} using gold nanoparticles cofunctionalized with 6-mercaptopicolinic acid and l-cysteine. *Analyst* 136:3725
- Kim S, Kim J, Lee NH, Jang HH, Han MS (2011) A colorimetric selective sensing probe for calcium ions with tunable dynamic ranges using cytidine triphosphate stabilized gold nanoparticles. *Chem Commun* 47:10299
- Zhang Y, Li B, Chen X (2010) Simple and sensitive detection of dopamine in the presence of high concentration of ascorbic acid using gold nanoparticles as colorimetric probes. *Microchim Acta* 168:107
- Lin YW, Huang CC, Chang HT (2011) Gold nanoparticle probes for the detection of mercury, lead and copper ions. *Analyst* 136:863
- Ai K, Liu Y, Lu L (2009) Hydrogen-bonding recognition-induced color change of gold nanoparticles for visual detection of melamine in raw milk and infant formula. *J Am Chem Soc* 131:9496
- Tan F, Liu X, Quan X, Chen J, Li X, Zhao H (2011) Selective detection of nanomolar Cr(VI) in aqueous solution based on 1,4-dithiothreitol functionalized gold nanoparticles. *Anal Method* 3:343
- Sun J, Ge J, Liu W, Fan Z, Zhang H, Wang P (2011) Highly sensitive and selective colorimetric visualization of streptomycin in raw milk using Au nanoparticles supramolecular assembly. *Chem Commun* 47:9888
- Han C, Zhang L, Li H (2009) Highly selective and sensitive colorimetric probes for Yb^{3+} ions based on supramolecular aggregates assembled from β -cyclodextrin-4,4'-dipyridine inclusion complex modified silver nanoparticles. *Chem Commun* 45:3545
- Zhang F, Zeng L, Zhang Y, Wang H, Wu A (2011) A colorimetric assay method for Co^{2+} based on thioglycolic acid functionalized hexadecyl trimethyl ammonium bromide modified Au nanoparticles (NPs). *Nanoscale* 3:2150
- Xu Y, Deng L, Wang H, Ouyang X, Zheng J, Li J, Yang R (2011) Metal-induced aggregation of mononucleotides-stabilized gold nanoparticles: an efficient approach for simple and rapid colorimetric detection of Hg(II). *Chem Commun* 47:6039
- Chansuvarn W, Imyim A (2012) Visual and colorimetric detection of mercury(II) ion using gold nanoparticles stabilized with a dithiadiazia ligand. *Microchim Acta* 1:57
- Li HB, Cui ZM, Han CP (2009) Glutathione-stabilized silver nanoparticles as colorimetric sensor for Ni^{2+} ion. *Sensor Actuat B-Chem* 143:87
- Li HB, Zhang LA, Yao Y, Han CP, Jin S (2010) Synthesis of azacrown ether-modified silver nanoparticles as colorimetric sensors for Ba^{2+} . *Supramol Chem* 22:544
- Cao Q, Zhao H, He Y, Li X, Zeng L, Ding N, Wang J, Yang J, Wang G (2010) Hydrogen-bonding-induced colorimetric detection of melamine by nonaggregation-based Au-NPs as a probe. *Biosens Bioelectron* 25:2680
- Kanayama N, Takarada T, Maeda M (2011) Rapid naked-eye detection of mercury ions based on non-crosslinking aggregation of double-stranded DNA-carrying gold nanoparticles. *Chem Commun* 47:2077
- Beqa L, Singh AK, Khan SA, Senapati D, Arumugam SR, Ray PC (2011) Gold nanoparticle-based simple colorimetric and ultrasensitive dynamic light scattering assay for the selective detection of Pb(II) from paints, plastics, and water samples. *ACS Appl Mater Inter* 3:668
- Zhang BH, Qi L, Wu FY (2010) Functionalized manganese-doped zinc sulfide core/shell quantum dots as selective fluorescent chemodosimeters for silver ion. *Microchim Acta* 170:147
- Li HB, Li FY, Han CP, Cui ZM, Xie GY, Zhang AQ (2010) Highly sensitive and selective tryptophan colorimetric sensor based on 4,4'-bipyridine-functionalized silver nanoparticles. *Sensor Actuat B-Chem* 145:194
- Su YH, Chang SH, Teoh LG, Chu WH, Tu SL (2009) Plasmons: chemical bonding coupling induced surface plasmon resonance splitting in self-assembled gold nanoparticles. *J Phys Chem C* 113:3923
- Yusa S, Fukuda K, Yamamoto T, Iwasaki Y, Watanabe A, Akiyoshi K, Morishima Y (2007) Salt effect on the heat-induced association behavior of gold nanoparticles coated with poly(N-isopropylacrylamide) prepared via reversible addition-fragmentation chain transfer (RAFT) radical polymerization. *Langmuir* 23:12842
- Bjerrum J, Schwarzenbach G (1958) Stability constants, *Chem Soc, London*
- Hung YL, Hsiung TM, Chen YY, Huang YF, Huang CC (2010) Colorimetric detection of heavy metal ions using label-free gold nanoparticles and alkanethiols. *J Phys Chem C* 114:16329
- Zhu D, Li X, Liu X, Wang J, Wang Z (2012) Designing bifunctionalized gold nanoparticle for colorimetric detection of Pb^{2+} under physiological condition. *Biosens Bioelectron* 31:505

33. Liu J, Lu Y (2003) A colorimetric lead biosensor using DNAzyme-directed assembly of gold nanoparticles. *J Am Chem Soc* 125:6642
34. Kim IB, Dunkhorst A, Gilbert J, Bunz UHF (2005) Sensing of lead ions by a carboxylate-substituted PPE: multivalency effects. *Macromolecules* 38:4560
35. Rabenstein DL, Fairhurst MT (1975) Nuclear magnetic resonance studies of the solution chemistry of metal complexes. XI. Binding of methylmercury by sulfhydryl-containing amino acids and by glutathione. *J Am Chem Soc* 97:2086
36. Wu SP, Chen YP, Sung YM (2011) Colorimetric detection of Fe³⁺ ions using pyrophosphate functionalized gold nanoparticles. *Analyst* 136:1887
37. Zhang J, Wang Y, Xu X, Yang X (2011) Specifically colorimetric recognition of calcium, strontium, and barium ions using 2-mercaptosuccinic acid-functionalized gold nanoparticles and its use in reliable detection of calcium ion in water. *Analyst* 136:3865